Naturally invariant measure of chaotic attractors and the conditionally invariant measure of embedded chaotic repellers

Buljan, Hrvoje; Paar, Vladimir

Naturally invariant measure of chaotic attractors and the conditionally invariant measure of embedded chaotic repellers

Hrvoje Buljan and Vladimir Paar
Department of Physics, Faculty of Science, University of Zagreb, PP 332, 10000 Zagreb, Croatia
(Received 13 October 2001; published 27 February 2002)

We study local and global correlations between the naturally invariant measure of a chaotic one-dimensional map f and the conditionally invariant measure of the transiently chaotic map f_H. The two maps differ only within a narrow interval H, while the two measures significantly differ within the images $f^l(H)$, where l is smaller than some critical number l_c. We point out two different types of correlations. Typically, the critical number l_c is small. The χ^2 value, which characterizes the global discrepancy between the two measures, typically obeys a power-law dependence on the width ϵ of the interval H, with the exponent identical to the information dimension. If H is centered on an image of the critical point, then l_c increases indefinitely with the decrease of ϵ, and the χ^2 value obeys a modulated power-law dependence on ϵ.

DOI: 10.1103/PhysRevE.65.036218 PACS number(s): 05.45.Ac, 05.45.Vx

I. INTRODUCTION

A picture of the asymptotic behavior of a permanently chaotic dissipative dynamical system is given by a strange attractor [1–3]. A more detailed description of the system involves the naturally invariant measure [1–7]. The naturally invariant measure provides information on the frequency of visits by typical trajectories to any given region on the attractor.

A picture of a transiently chaotic system is given by an invariant nonattracting chaotic set, called the chaotic repeller [8–13]. A trajectory starting close to the repeller exhibits erratic motion practically indistinguishable from the motion on the chaotic attractor for a long time. After the chaotic transient period, the trajectory escapes to some (possibly nonchaotic) attractor [8–13]. Some regions of the phase space containing the repeller are more likely to be visited by long lived chaotic transients than others. This likelihood is described in terms of the conditionally invariant measure, also referred to as the c measure [8–10,14–17].

The conditionally invariant measure was invented and interpreted by Pianigiani and Yorke in Ref. [14]. A rigorous mathematical analysis of the c measures can be found in Refs. [14–17]. Their existence and uniqueness has been established for a broad class of systems [14–17]. The c measure (call it μ_C) is not invariant under the systems dynamics, say a transiently chaotic map f_H. Instead, its image under f_H is proportional to itself:

$$\mu_C(f_H^{-1}(B)) = \exp(-\alpha)\,\mu_C(B), \tag{1}$$

where B denotes a set in the phase space, whereas α denotes the escape rate of chaotic transients from the repeller [8,9]. Equation (1) can be utilized for the calculation of the escape rate from the strange sets [8,9].

Let us define the problem studied in this paper. We consider unimodal maps on the interval, $f(x)$: $I \to I \subset \mathbb{R}$, with a smooth quadratic maximum assumed at a critical point x_c. We assume that f is chaotic, with a chaotic attractor A, and a naturally invariant measure μ_N. The information dimension of the attractor A is $D_1 = 1$.

Let $H = (\xi - \epsilon/2, \xi + \epsilon/2)$ be an interval on the attractor such that $\mu_N(H) > 0$. The region H will be referred to as the hole. Due to ergodicity, a trajectory started from a random initial condition will eventually enter the hole H [2]. However, there is a set of points on A yielding trajectories that never enter this region. This set of points is a chaotic repeller (call it R) embedded within the attractor A [18–20]. Chaotic repellers embedded within chaotic attractors arise in the context of communicating with chaos [18–20].

Since chaotic repellers are typically associated with transient chaos, we may ask: Is there a transiently chaotic map to which the embedded repeller R corresponds? The repeller R governs the dynamics of the transiently chaotic map with a hole [14–22],

$$f_H(x) = \begin{cases} f(x), & x \in I \setminus H \\ \text{outside of } I, & x \in H. \end{cases} \tag{2}$$

Here, μ_C denotes the c measure corresponding to the map f_H, and the embedded chaotic repeller R.

In many physical or numerical experiments, the phase space is covered with cells from a fine grid, and probability measures are visualized and analyzed by using such grids [1–3,7,8,23]. Imagine that we cover the interval I with bins B from a grid of unit size $\epsilon_B \leqslant \epsilon$. In this paper, the correlation between the naturally and the conditionally invariant measure is analyzed by using such a grid. Local correlations are described in terms of the relative local difference

$$\delta_r(B) = \frac{|\mu_C(B) - \mu_N(B)|}{\mu_N(B)}. \tag{3}$$

A quantitative description of the global discrepancy between the two measures is characterized in terms of the χ^2 value

$$\chi^2(\xi, \epsilon, \epsilon_B) = \sum_B \frac{[\mu_C(B) - \mu_N(B)]^2}{\mu_N(B)} = \sum_B |\delta_r(B)\,\delta(B)|, \tag{4}$$

where $\delta(B) = \mu_C(B) - \mu_N(B)$ [24]. The outline of the manuscript and the main results are as follows.

In Sec. II, we present numerical analysis demonstrating that in most of the bins that cover the attractor, $\delta_r(B) \simeq 0$. Significant differences between the two measures occur within the first l_c images of the hole H, where l_c denotes some critical number. In other words, $\delta_r(B)$ is significantly larger than zero for $B \subset f^l(H)$, $0 < l \leqslant l_c$. These differences will be referred to as the gross differences between the two measures. Since the number of bins that cover the first l_c images of the hole is $\sim \epsilon/\epsilon_B$, the resolution with which the gross differences are observed is given in terms of the ratio $\eta = \epsilon/\epsilon_B \geqslant 1$, also referred to as the grid-refinement parameter. The fine differences between the two measures may occur at the iterates of the critical point.

In Sec. III we discuss the way in which the fine differences emerge in the histogram representing $\delta_r(B)$ with the increase of the grid-refinement parameter η. We will show that the fine differences appear as sharp, isolated spikes in the $\delta_r(B)$ histogram.

In Sec. IV, we present the main results of this manuscript. The gross differences are studied analytically. We will demonstrate the existence of two types of gross differences between the two measures.

(1) If ξ is a typical point on the attractor, then the critical number l_c is small, and independent of $\epsilon \ll 1$. The critical number l_c is determined by the rate at which the images of the hole get stretched under the systems dynamics. The magnitude of the global discrepancy between the two measures is correlated with the visiting frequency by typical trajectories to the hole, $\chi^2 \sim \mu_N(H)$. As a consequence, the χ^2 value obeys a power-law dependence on the size of the hole, $\chi^2_{\xi\eta}(\epsilon) \sim \epsilon^{D_1}$. (The parameters ξ and η are written as indices since they are held constant.)

(2) When the point ξ is not typical, a different type of correlation may occur. If ξ lies on an image of the critical point x_c, then the magnitude of l_c is primarily determined by the size of the hole ϵ. The critical number increases approximately logarithmically with the decrease of ϵ, i.e., $l_c(\epsilon) \sim \ln(1/\epsilon)$. Consequently, the χ^2 value obeys a modulated power-law dependence on ϵ: $\chi^2_{\xi\eta}(\epsilon) \sim \ln(1/\epsilon)\epsilon^{D_{\mu_N}(\xi)}$, where $D_{\mu_N}(\xi)$ denotes the pointwise dimension of μ_N at ξ.

In Sec. V we present the main conclusions of this paper.

II. NUMERICAL COMPARISON OF μ_N AND μ_C

Let us recall the definition of the naturally and the conditionally invariant measures corresponding to the original map f, and the modified map f_H, respectively. Imagine a smooth initial probability measure $\mu^{(0)}$ on the interval I, $\mu^{(0)}(I) = 1$. The evolution of $\mu^{(0)}$ under the map f leads to the measures $\mu_N^{(1)}, \mu_N^{(2)}, \ldots, \mu_N^{(T)}, \ldots$, and finally to the naturally invariant measure of the map f, $\lim_{T\to\infty} \mu_N^{(T)} = \mu_N$, $\mu_N(I) = 1$ [1–5].

The evolution of $\mu^{(0)}$ under the map f_H leads to the measures $\mu_C^{(1)}, \mu_C^{(2)}, \ldots, \mu_C^{(T)}, \ldots$. Consider the action of the map f_H on the measure $\mu_C^{(T)}$, $T \geqslant 0$. The content of $\mu_C^{(T)}$ within the hole H $[\mu_C^{(T)}(H)]$ is mapped outside of the interval I. Imagine that we multiply the resulting measure $\mu_C^{(T+1)}$ by $[1 - \mu_C^{(T)}(H)]^{-1}$. This procedure asserts that $\mu_C^{(T+1)}(I) = 1$, $\forall\ T \geqslant 0$. In the limit $T \to \infty$, the measure $\mu_C^{(T)}$ converges to the conditionally invariant measure μ_C of the map f_H, while $[1 - \mu_C^{(T)}(H)]^{-1}$ converges to the constant $\exp \alpha$ (α denotes the escape rate from the repeller R, see Eq. (1) and Refs. [8,9,14–17]).

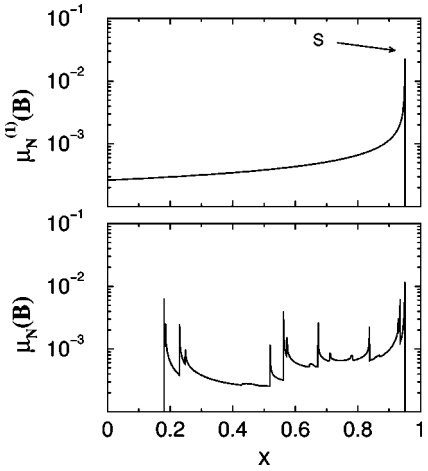

FIG. 1. (a) The first image of a uniform probability measure under the map f represented by a histogram. (b) The content of the naturally invariant measure within a bin B, against the position of the bin x. The size of the bins is $\epsilon_B = 5 \times 10^{-4}$.

Figures 1 and 2 illustrate the action of the original map f,

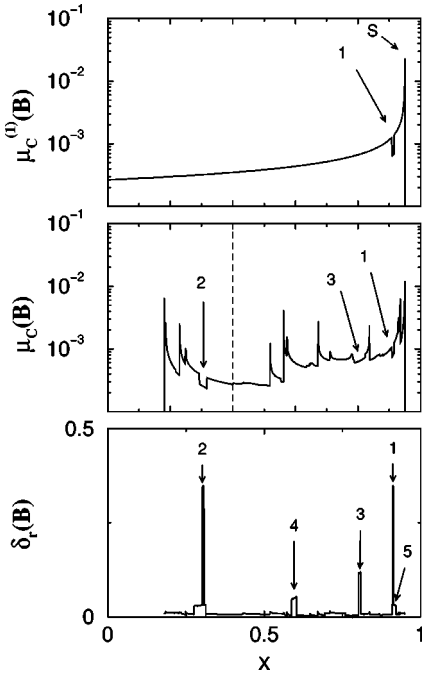

FIG. 2. (a) The image of a uniform probability measure under the map f_H represented by a histogram. (b) The content of the c measure within a bin B against the position of the bin x. (c) $\delta_r(B)$ against the position of the bin. The positions of the first five images of H are indicated by arrows. The parameters corresponding to the figures are as follows: For (a) and (b) $\xi = 0.4$, $\eta = 20$, and $\epsilon = 0.01$. For (c) $\xi = 0.4$, $\eta = 20$, and $\epsilon = 0.002$.

and of the modified map f_H, respectively, on a uniform initial probability measure $\mu^{(0)}$. For all illustrations we utilize the logistic map $f(x)=rx(1-x)$, at the parameter value $r=3.8$. Parameters ξ and ϵ defining the modified map(s) are written in captions. Figures 1(a) and 2(a) display the first images of the uniform measure $\mu^{(0)}$ under the maps f and f_H, respectively. Figures 1(b) and 2(b) display the naturally and the conditionally invariant measure, respectively. Finally, Fig. 2(c) displays the relative local difference $\delta_r(B)$ against the position of the bin B.

We observe the following.

(i) The content of $\mu^{(0)}$ within the hole H $[\mu^{(0)}(H)]$ is mapped outside of the interval $I=[0,1]$ by the modified map f_H. Hence, the measures $\mu_C^{(1)}$ and $\mu_N^{(1)}$ significantly differ within the image $f^1(H)$. The evolution of $\mu_C^{(1)}$ propagates these differences at successive images of the hole H [see Figs. 2(b) and 2(c)]. From Fig. 2(c) we see that the c measure displayed in Fig. 2(b) significantly differs from the naturally invariant measure only within a few successive images of the hole H.

(ii) Since f has a smooth maximum at x_c, at the image of the critical point $f(x_c)$, both $\mu_N^{(1)}$ and $\mu_C^{(1)}$ have a spike. The spike is labeled by the letter S in Figs. 1(a) and 2(a). The evolution of the measures $\mu_N^{(1)}$ and $\mu_C^{(1)}$ propagates the spike at the iterates of the critical point [see Figs. 1(b) and 2(b)].

From a number of similar numerical experiments that have been performed it follows that if $\epsilon \ll 1$, the relative local difference $\delta_r(B) \simeq 0$ in most of the bins B. The gross differences between the two measures are found within the first l_c images of the hole, where l_c denotes some critical number. In other words, if $B \subset f^l(H)$, where $l \leqslant l_c$, then $\delta_r(B)$ is significantly larger than zero [see Fig. 2(c)]. In most cases (but not necessarily) l_c is a small number.

To see the meaning of the grid-refinement parameter η, consider the number of bins that cover the lth image of the hole $f^l(H)$, $l \leqslant l_c$. For $\epsilon \ll 1$, the length interval $f^l(H)$ is approximately $\Lambda^l(\xi)\epsilon$, where $\Lambda^l(\xi) \equiv |df^l(x)/dx|_{x=\xi}$. Therefore, $f^l(H)$ is covered with approximately $\Lambda^l(\xi)\epsilon/\epsilon_B = \Lambda^l(\xi)\eta$ bins B. Thus, for larger values of η, the gross differences between the two measures are resolved with higher resolution. It follows that by keeping the grid-refinement parameter $\eta=\epsilon/\epsilon_B$ fixed, the differences between the two measures (e.g., the χ^2 value) can be studied as a function of the size of the hole ϵ with effectively constant resolution. In most calculations presented here, we find it sufficient to use the value $\eta=20$.

Let $k_{x_c \to H} \geqslant 0$ denote the number of iterates it takes for the critical point x_c to be mapped to the hole H. In other words, if $x_c \in H$, $k_{x_c \to H}=0$; if $x_c \notin H$, then for $0 \leqslant k' < k_{x_c \to H}$, $f^{k'}(x_c) \notin H$, and $f^{k_{x_c \to H}}(x_c) \in H$. The measure μ_N has a spike at every iterate of x_c under the map f, whereas μ_C has only $k_{x_c \to H}$ spikes that are located at the iterates $f^{k'}(x_c)$, $k'=1,2,\ldots,k_{x_c \to H}$. As an illustration, the c measure displayed in Fig. 3(a) has only two spikes since $k_{x_c \to H}=2$. Therefore, it is possible that the c measure, unlike the naturally invariant measure, does not have spikes at the iterates of the critical point $f^{k'}(x_c)$, $k' > k_{x_c \to H}$. These differences are referred to as the fine differences between the two measures.

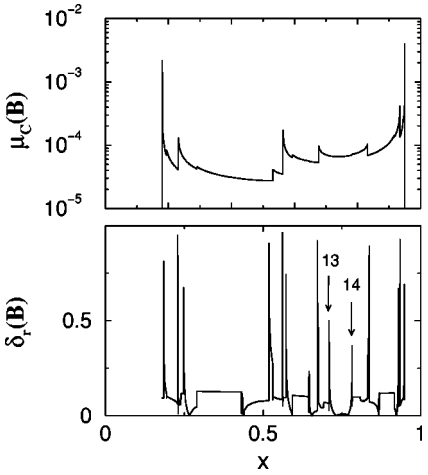

FIG. 3. (a) The histogram representing the c measure defined by the parameters $\xi=0.1805$, $\epsilon=0.001$, $\eta=20$, and $\epsilon_B=\epsilon/\eta=5\times10^{-5}$. The c measure has only two spikes, at $f(x_c)$ and at $f^2(x_c)=\xi$. (b) $\delta_r(B)$ against the position of the bin. An inspection of the differences shows that the gross differences appear within the first $l_c \sim 8$–9 images of H. The fine differences at $f^{13}(x_c)$ and $f^{14}(x_c)$ are indicated by arrows.

III. FINE DIFFERENCES BETWEEN μ_N AND μ_C

To what extent will the fine differences be resolved depends on the grid-refinement parameter η and the integer $k_{x_c \to H}$. In order to demonstrate this, suppose that x_c is not eventually periodic. Although the naturally invariant measure has infinite number of spikes, only a finite number of them will be seen on a histogram representing μ_N (see Ref. [3] or Ref. [1], p. 54). To be more specific, the histogram resolves only spikes at the iterates $f^{k'}(x_c)$, $k' \leqslant k_c$, where k_c denotes some critical value. With the decrease of the size of the bins ϵ_B, i.e., with the increase of the grid-refinement parameter η (parameters ξ and ϵ are kept constant), the critical value k_c increases indefinitely [1,3]. The c measure has spikes only at the iterates $f^{k'}(x_c)$, $k' < k_{x_c \to H}$. Therefore, in order to resolve the fine differences on a grid, η has to be large enough so that $k_c > k_{x_c \to H}$. Now, consider the bins that cover the iterates $f^{k'}(x_c)$, $k_{x_c \to H} < k' \leqslant k_c$. Since μ_N has spikes at these points, and μ_C does not, $\mu_N(B) \geqslant \mu_C(B)$, and $\delta_r(B) \simeq 1$.

As an illustration of the fine differences between the two measures, Fig. 3(b) displays $\delta_r(B)$ corresponding to the c measure in Fig. 3(a). Since $k_{x_c \to H}=2$ is small, the condition $k_c > k_{x_c \to H}$ which is required for the observation of fine differences is satisfied already for $\eta=20$. The critical number of the images of the hole H where μ_C grossly differs from μ_N is approximately $l_c=8$–9. However, within some bins B that are not located at the first l_c images of the hole we see significant $\delta_r(B)$ values. These bins cover the spikes at the

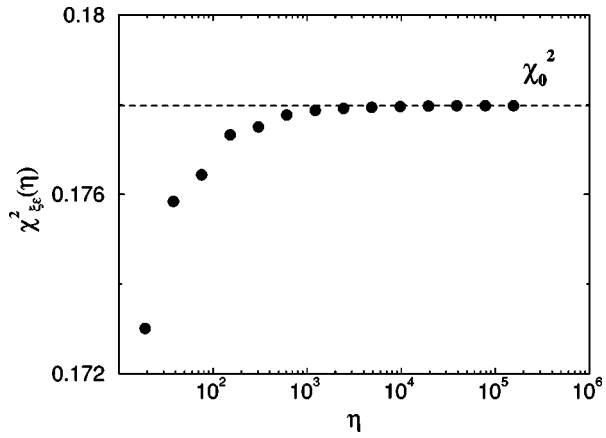

FIG. 4. The $\chi^2_{\xi\epsilon}(\eta)$ value against η. The position of the hole is $\xi=0.95=f(x_c)$, whereas the size of the hole $\epsilon=0.01$.

points $f^{k'}(x_c)$, $k'=10,\ldots,14$, $k'>k_{x_c\to H}=2$. These fine differences typically appear as sharp, isolated spikes in a histogram representing $\delta_r(B)$.

In Fig. 2(c) the fine differences are not resolved. Since $k_{x_c\to H}$ corresponding to Fig. 2(c) is large ($k_{x_c\to H}=4150$), the condition $k_c>k_{x_c\to H}$ can be satisfied only for extremely large value of the grid-refinement parameter η. For that reason, we are in this case unable to numerically calculate and draw the histogram representing $\delta_r(B)$, which would resolve the fine differences.

Let us consider behavior of the global discrepancy between the two measures $\chi^2_{\xi\epsilon}(\eta)$ in dependence of the grid-refinement (ξ and ϵ are held fixed). With the increase of η, the grid resolves more fine differences between the two measures, and the $\chi^2_{\xi\epsilon}(\eta)$ value increases. Figure 4 displays the χ^2 value in dependence on η. This numerical experiment suggests that in the limit $\eta\to\infty$, the $\chi^2_{\xi\epsilon}(\eta)$ value converges to some limiting value $\chi^2_0(\xi,\epsilon)$. This result can be explained as follows. In the limit $\eta\to\infty$, the sum in Eq. (4) is substituted by the integral, and the measures μ_N and μ_C by the naturally and the conditionally invariant density, respectively. Therefore, given the map f, the quantity $\chi^2_0(\xi,\epsilon)$ is determined by the position and the size of the hole.

The analysis of the following section utilizes the concept of the pointwise dimension. The pointwise dimension of a probability measure μ at the point x is defined as [1,23]

$$D_\mu(x)=\lim_{\epsilon_B\to 0}\frac{\ln\mu(B(x))}{\ln\epsilon_B}, \tag{5}$$

where $B(x)=(x-\epsilon_B/2,x+\epsilon_B/2)$. Let us compare the pointwise dimension of μ_N and μ_C at some point on the attractor A. The pointwise dimension of μ_N at almost every point $x\in A$ (with respect to the naturally invariant measure) is $D_{\mu_N}(x)=D_1=1$. The pointwise dimension of μ_N differs from D_1 only at the positions of the spikes. Since the maximum of the map f at the critical point is quadratic, $D_{\mu_N}(f^{k'}(x_c))=1/2$, where $k'=1,2,\ldots$ [1]. Similarly, the pointwise dimension of μ_C is 1 everywhere, except at the positions of the spikes. Since the spikes of μ_C are located only at the first $k_{x_c\to H}$ iterates of x_c, $D_{\mu_C}(f^{k'}(x_c))=1/2$, for $k'=1,2,\ldots,k_{x_c\to H}$.

IV. GROSS DIFFERENCES BETWEEN μ_N AND μ_C

In this section, for some fixed value of the parameters ξ and η, and for sufficiently small size of the hole ϵ, we estimate analytically, and calculate numerically the relative local difference $\delta_r(B)$, and the χ^2 value. This provides an analytical description of the gross differences between the two measures.

At first, we qualitatively discuss the transition from the c measure to the naturally invariant measure that occurs when ϵ is reduced to zero. From the definition of the embedded repeller R it follows that $R\subset A$. As ϵ decreases to zero, the embedded repeller R gradually becomes identical to the attractor A, the measure μ_C becomes gradually identical to the measure μ_N, while Eq. (1) transforms into

$$\mu_N(B)=\mu_N(f^{-1}(B)). \tag{6}$$

Thus, if ϵ is sufficiently small, then $\mu_C(B)\simeq\mu_N(B)$ in most of the bins B [compare Figs. 1(b) and 2(b)].

In order to make the exposition clear, two definitions are introduced. Consider a subset of the phase space, $P\subset I$. Let $l_{H\to P}$ denote the smallest positive integer l for which the section $f^l(H)\cap P\neq\emptyset$. Let the quantity $\delta(P)$ denote the difference between the two measures within the set P: $\delta(P)=\mu_C(P)-\mu_N(P)$.

The relative local difference within a particular bin B depends on the number of iterates it takes for the hole H to map to the bin B, i.e., $l_{H\to B}$. In order to present $\delta_r(B)$ in the form suitable for the analysis, from Eqs. (1) and (6) we write

$$\mu_C(B)\simeq\mu_C(f_H^{-l_{H\to B}}(B)), \tag{7}$$

and

$$\mu_N(B)=\mu_N(f^{-l_{H\to B}}(B)\cap H)+\mu_N(f_H^{-l_{H\to B}}(B)). \tag{8}$$

Equation (7) follows from the approximation $e^{l_{H\to B}/\tau}\simeq 1+l_{H\to B}/\tau\simeq 1$. The largest integer $l_{H\to B}$ associated with some bin(s) scales as $l_{H\to B}\sim\ln(1/\epsilon)$ for $\epsilon\ll 1$ [25], whereas the lifetime τ scales as $\tau\sim\epsilon^{-D_{\mu_N}(\xi)}$ [1,12,25]. Hence, the approximation $e^{l_{H\to B}/\tau}\simeq 1$ is valid for every bin B as long as $\epsilon\ll 1$. By subtracting Eqs. (7) and (8) we obtain

$$\delta(B)\simeq-\mu_N(f^{-l_{H\to B}}(B)\cap H)+\delta(f^{-l_{H\to B}}(B)\setminus H), \tag{9}$$

and

$$\delta_r(B)\simeq\frac{|-\mu_N(f^{-l_{H\to B}}(B)\cap H)+\delta(f^{-l_{H\to B}}(B)\setminus H)|}{\mu_N(B)}. \tag{10}$$

The functional dependence of $\delta(B)$ [and consequently $\delta_r(B)$] on $l_{H\to B}$ is investigated by studying the two terms on the right-hand side of Eq. (9). In the following subsections

we report two types of gross differences between the two measures, i.e., we present two types of dependences of $\delta_r(B)$ on $l_{H\to B}$.

A. Typical correlations

If ξ is chosen at random, by using the naturally invariant measure, then the orbit originating from ξ is typical in the sense that $D_{\mu_N}(f^{l'}(\xi))=D_1=1$, $\forall l'\geqslant 0$. Consequently, $D_{\mu_C}(f^{l'}(\xi))=D_1=1$, $\forall l'\geqslant 0$ (see Sec. III).

Consider the bins for which $l_{H\to B}=l$ $(l>0)$. Since $D_{\mu_N}(\xi)=1$, for sufficiently small ϵ, the first term on the right-hand side of Eq. (9) can be written as $\mu_N(f^{-l}(B)\cap H)\sim \epsilon_B/\Lambda^l(\xi)$, where $\Lambda^l(\xi)=|f'(\xi)f'(f^1(\xi))\cdots f'(f^{l-1}(\xi))|=|df^l(x)/dx|_{x=\xi}$. Due to the chaoticity of the map, the quantity $\Lambda^l(\xi)$ increases very rapidly with the increase of l. In fact, since ξ is a typical point, for large enough l the quantity $\Lambda^l(\xi)\sim e^{\lambda l}$, where λ denotes the Lyapunov exponent of the map. Thus, if the map is more chaotic, the quantity $\mu_N(f^{-l}(B)\cap H)$ should decrease more rapidly with the increase of l.

Consider the second term on the right-hand side of Eq. (9). Let us observe the set $f_H^{-l}(B)$ and the value of $\delta(f_H^{-l}(B))$ in dependence of l. $f_H^{-l}(B)$ is a union of small disjoint intervals that map their measure to B in l iterates. Due to the chaoticity of the map f, the number of these intervals grows exponentially fast with the increase of l, and they are distributed all over the attractor. Thus, the set $f_H^{-l}(B)$ becomes more democratic with the increase of l in a sense that the quantity $\delta(f_H^{-l}(B))$ reflects the global agreement between the two measures. If the map is more chaotic, the number of disjoint intervals that $f_H^{-l}(B)$ is made of grows at a faster rate with the increase of l [20]. Thus, depending on the chaoticity of the map, the quantity $\delta(f_H^{-l}(B))$ will be approximately equal to zero already for small values of l.

From this discussion of the two terms on the right-hand side of Eq. (9), we conclude that $\delta(B)$ [and consequently $\delta_r(B)$] can be significantly different from zero only for small values of l. In other words, the critical value l_c is typically small [see Fig. 2(c)].

Let us make an estimate of the relative local difference $\delta_r(B)$. Generally, the depth of the lth well $\delta(B)$ is described by the following formula:

$$\begin{aligned}\delta(B)=&-\mu_N(f^{-l}(B)\cap H)-\mu_N(f^{-l_1}(f_H^{-l}(B))\cap H)\\&-\mu_N(f^{-l_2}(f_H^{-(l+l_1)}(B))\cap H)-\cdots\\&-\mu_N(f^{-l_{n+1}}(f_H^{-(l+l_1+\cdots+l_n)}(B))\cap H),\end{aligned}\tag{11}$$

where $l_1\equiv l_{H\to f_H^{-l}(B)}$, $l_2\equiv l_{H\to f_H^{-(l+l_1)}(B)}$, $\ldots$, $l_{n+1}\equiv l_{H\to f_H^{-(l+l_1+\cdots+l_n)}(B)}$. The integer n is chosen such that $l+l_1+\cdots+l_n\leqslant l_c$, while $l+l_1+\cdots+l_n+l_{n+1}>l_c$, i.e., $\delta(f_H^{-(l+l_1+\cdots+l_n+l_{n+1})}(B))\simeq 0$. From this it follows that $n\leqslant l_c$, i.e., the number of terms in Eq. (11) is small.

Since the hole is narrow ($\epsilon\ll 1$), and since the critical number l_c is small, it is most likely that the set $f_H^{-l}(B)$ does not overlap the first l_c images of the hole H, i.e., most likely $l_{H\to f_H^{-l}(B)}>l_c$. In fact, if the first $2l_c$ images of the hole do not overlap, i.e., if $f^{l_1}(H)\cap f^{l_2}(H)=\varnothing$ for $l_1,l_2\leqslant 2l_c$ $(l_1\neq l_2)$, it can be shown that $l_{H\to f_H^{-l}(B)}>l_c$, and consequently $\delta(f_H^{-l}(B))\simeq 0$. Since ξ is a typical point, it is not eventually periodic, and the condition $f^{l_1}(H)\cap f^{l_2}(H)=\varnothing$ for $l_1,l_2\leqslant 2l_c$ $(l_1\neq l_2)$ can be satisfied just by making ϵ to be sufficiently small. Therefore, in the typical case, the relative local difference is approximately

$$\delta_r(B)\simeq\frac{\mu_N(f^{-l}(B)\cap H)}{\mu_N(B)}.\tag{12}$$

We have already seen that the quantity $\mu_N(f^{-l}(B)\cap H)$ decreases approximately exponentially fast with the increase of l, $\mu_N(f^{-l}(B)\cap H)\sim 1/\Lambda^l(\xi)$. Therefore, the relative local difference decreases rapidly with the increase of l. The critical number l_c is determined by how rapidly $\Lambda^l(\xi)$ increases with the increase of l, i.e., l_c depends on the rate at which the images of the hole get stretched by the dynamics of the map f. Since, $\mu_N(f^{-l}(B)\cap H)\sim\mu_N(B)\sim\epsilon^{D_1}$, both $\delta_r(B)$ and l_c are independent of ϵ.

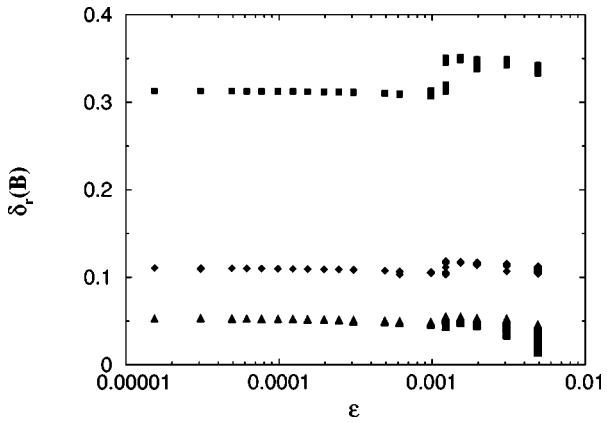

FIG. 5. The relative local difference $\delta_r(B)$ against ϵ. The bins B are located at successive images of the hole: $B\subset f^2(H)$ (squares), $B\subset f^3(H)$ (diamonds), and $B\subset f^4(H)$ (triangles). The position of the hole $\xi=0.40$ $[D_{\mu_N}(\xi)=1]$, and the grid-refinement parameter $\eta=20$ are kept constant.

As an illustration, Fig. 5 displays $\delta_r(B)$ as a function of ϵ for the bins located at the lth image of the hole H. Note that in this typical case, for $\epsilon\ll 1$, $\delta_r(B)$ is practically independent of the position of the bin within $f^l(H)$, $l\leqslant l_c$. This is consistent with Eq. (12).

Let us make an estimate of the χ^2 value. Most of the contributions to the χ^2 value come from the bins located within the first l_c images of the hole H. Therefore,

$$\begin{aligned}\chi^2_{\xi\eta}(\epsilon)&\simeq\sum_{l'=1}^{l_c}\sum_{B\subset f^{l'}(H)}|\delta_r(B)\delta(B)|\\&\simeq\sum_{l'=1}^{l_c}\overline{\delta_r}(l')\sum_{B\subset f^{l'}(H)}\mu_N(f^{-l'}(B)\cap H)\\&\simeq\mu_N(H)\sum_{l'=1}^{l_c}\overline{\delta_r}(l')\sim\epsilon^{D_{\mu_N}(\xi)}.\end{aligned}\tag{13}$$

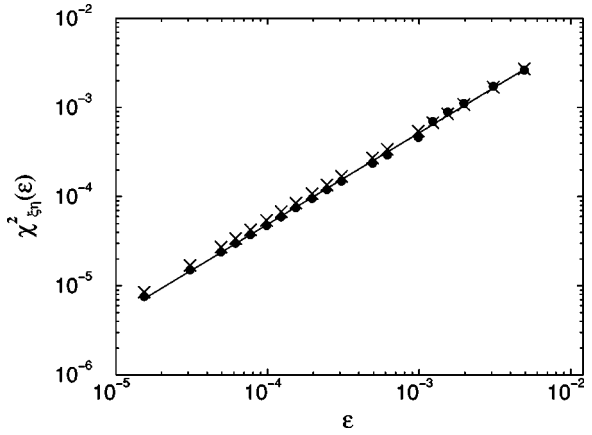

FIG. 6. The $\chi^2_{\xi\eta}(\epsilon)$ value against ϵ (closed circles). The hole is positioned at $\xi=0.4$, $D_{\mu_N}(\xi=0.4)=1$. The grid-refinement parameter $\eta=20$. The quantity $\mu_N(H)$ against ϵ is labeled by the letters *x*.

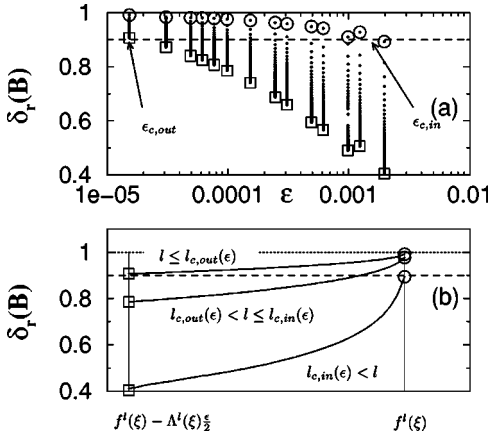

FIG. 7. (a) The relative local difference $\delta_r(B)$ for the bins $B \subset f^3(H)$ against ϵ. The parameters $\xi = f^1(x_c) = 0.95$ and $\eta = 20$ are kept constant. (b) The appearance of $\delta_r(B)$ for the bins B that are within the interval $(f^l(\xi) - \Lambda^l(\xi)\epsilon/2, f^l(\xi))$. The appearance is shown for $l < l_{c,out}(\epsilon)$, $l_{c,out}(\epsilon) < l < l_{c,in}(\epsilon)$, and $l_{c,in}(\epsilon) < l$. The quantities $\delta_r(B_{in})$ and $\delta_r(B_{out})$ are marked by open circles and open squares, respectively.

In the first line of Eq. (13) we have assumed that the first l_c images of the hole do not overlap. The second line follows from the fact that for $\epsilon \ll 1$, the quantity $\delta_r(B)$ is practically independent of the position of the bin B within the l'th image [see Figs. 2(c) and 5], i.e., $\delta_r(B) \simeq \overline{\delta_r}(l')$, where $\overline{\delta_r}(l')$ denotes the average value of the relative local difference within the image $f^{l'}(H)$. The third line in Eq. (13) follows from the approximation $\Sigma_{B \subset f^{l'}(H)} \mu_N(f^{-l'}(B) \cap H) \simeq \mu_N(H)$. This approximation is very accurate if the grid-refinement parameter η is large enough. From Eq. (13) it follows that if $\mu_N(H)$ is larger, the global discrepancy between the two measures will be larger as well. Furthermore, since $\overline{\delta_r}(l')$ is independent of ϵ, the $\chi^2_{\xi\eta}(\epsilon)$ value obeys a power-law dependence on ϵ. [Note that the power-law follows only from the condition $D_{\mu_N}(f^{l'}(\xi)) = D_1 = 1$, and the fact that l_c is independent of ϵ. In other words, it is not necessary that the first $2l_c$ images of the hole do not overlap.]

Figure 6 displays a test of Eq. (13) for the logistic map ($r=3.8$). We see that the visiting frequency by typical trajectories to the hole, $\mu_N(H)$, determines the magnitude of the global discrepancy between the two measures. Note that in this particular case $\Sigma_{l'=1}^{l_c} \overline{\delta_r(l')} \simeq 1$ [see Fig. 2(c)], i.e., $\chi^2 \simeq \mu_N(H)$. The points were fitted to the functional dependence $A_0 \epsilon^{A_1}$. The fitted value of the exponent A_1 is $A_1 = 1.027 \pm 0.008$, which is in good agreement with prediction $A_1 = D_{\mu_N}(\xi) = 1$ [see Eq. (13)]. This shows that the approximations leading to Eq. (13) are good.

B. Correlations for $\xi = f^k(x_c)$

If the position of the hole ξ lies on an atypical point, a completely different type of correlation between the two measures may occur. In this subsection, we consider the case when ξ lies on an image of the critical point, $f^k(x_c) = \xi$, $k \geqslant 1$. Thus, $D_{\mu_N}(\xi) = 1/2 \neq D_1$. We assume that $k \equiv k_{x_c \to H}$.

Consider the bins for which $l_{H \to B} = l$ ($l > 0$). These bins are located at the lth image of the hole H, i.e., they are grouped around the point $f^l(\xi) = f^{k+l}(x_c)$. The naturally invariant measure has a spike at $f^{k+l}(x_c)$. The spike is usually oriented to the left or to the right of an image of the critical point. For example, the spike at $f(x_c) = 0.95$ in Fig. 1(b) is oriented to the left, whereas the spike at $f^2(x_c) = 0.1805$ in Fig. 1(b) is oriented to the right. The spike can also have approximately symmetrical shape, e.g., when x_c maps to the unstable fixed point in two iterates (see Fig. 8 in Ref. [2]). Without losing any generality, we assume that the spike at $f^{k+l}(x_c)$ is oriented to the left of $f^{k+l}(x_c)$.

Consider the bins that are to the right of $f^l(\xi)$. For sufficiently small $\epsilon = \eta \epsilon_B$, the two measures have the same scaling behavior, $\mu_N(B) \sim \epsilon_B \sim \mu_C(B)$, and the analysis can be reduced to the one from the preceding subsection.

To study the correlation between the two measures within the bins to the left of $f^l(\xi)$, we must study the scaling of the terms in Eqs. (7) and (8) with ϵ_B. As the size of the hole $\epsilon = \eta \epsilon_B$ is reduced, the sets B and $f^{-l}(B) \cap H$ get closer to the tip of the spike at $f^l(\xi)$ and ξ, respectively. Therefore, $\mu_N(B) \sim \mu_N(f^{-l}(B) \cap H) \sim \epsilon_B^{1/2}$. If the spike of μ_N at the point $f^l(\xi)$ originates only from the spike at ξ, then $\mu_N(f_H^{-l}(B)) \sim \epsilon_B$. Consequently, $\mu_C(f_H^{-l}(B)) \sim \epsilon_B$, and $\mu_C(B) \sim \epsilon_B$. Hence, no matter how large l is, for sufficiently small ϵ, $\mu_N(B) \sim \epsilon^{1/2} \gg \epsilon \sim \mu_C(B)$, i.e., $\delta_r(B) \simeq 1$. In other words, we can find some critical value $\epsilon_c(l)$, such that for $\epsilon < \epsilon_c(l)$, the quantity $\delta_r(B) > p_t$, where p_t denotes some "threshold value" close to 1 (e.g., $p_t = 0.90$).

There are approximately $\Lambda^l(\xi)\epsilon/2$ bins that are within $f^l(H)$, and are to the left of $f^l(\xi)$. As ϵ is reduced, $\delta_r(B)$ corresponding to every one of these bins approaches the value $\delta_r(B) = 1$. However, the relative local difference $\delta_r(B)$ within the bins B that are closer to the tip of the spike will become larger than the "threshold value" p_t for smaller values of ϵ. As an illustration, Fig. 7(a) displays the dependence of $\delta_r(B)$ on ϵ for $B \subset f^3(H)$ ($l=3$). We see that the critical value $\epsilon_{c,out}(l)$ corresponding to the outermost bin B_{out}, is

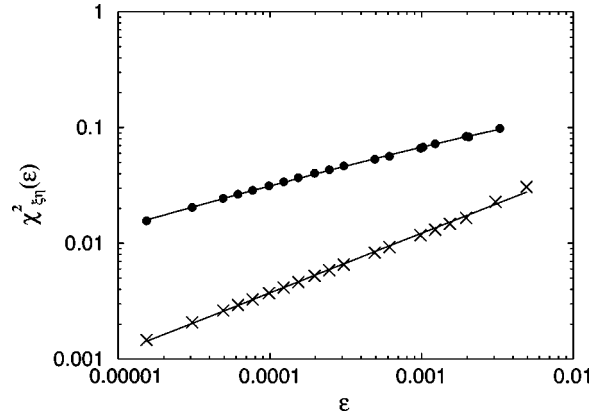

FIG. 8. The $\chi^2_{\xi\eta}(\epsilon)$ value against ϵ (closed circles). The hole is positioned at the first image of the critical point, i.e., $\xi=f(x_c)=0.95$, $D_{\mu_N}(\xi=0.95)=1/2$. The grid-refinement parameter $\eta=20$. The quantity $\mu_N(H)$ against ϵ is labeled by the letters *x*.

much smaller than the critical value $\epsilon_{c,in}(l)$ corresponding to bin B_{in} that is adjacent to the tip of the spike, $\epsilon_{c,out}(l)<\epsilon_{c,in}(l)$. In the Appendix, it is shown that the critical values $\epsilon_{c,in}(l)$ and $\epsilon_{c,out}(l)$ decrease very rapidly (approximately exponentially fast) with the increase of l.

Inversely, the number of the successive images of the hole where the two measures significantly differ increases (approximately logarithmically) with the decrease of ϵ. Let $l_{c,out}(\epsilon)$ $[l_{c,in}(\epsilon)]$ denote the critical number of the images of the hole, such that for $l<l_{c,out}(\epsilon)$ $[l<l_{c,in}(\epsilon)]$, the relative local difference is larger than the threshold value, i.e., $\delta_r(B_{out})>p_t$ $[\delta_r(B_{in})>p_t$, respectively]. From the dependence of the critical values ϵ_c on l, it follows that $l_{c,in}(\epsilon)\sim 2l_{c,out}(\epsilon)\sim\lambda(\xi)^{-1}\ln(1/\epsilon)$ [see Eqs. (A4) and (A5) in the Appendix]; the quantity $\lambda(\xi)$ denotes the Lyapunov exponent for initial condition ξ. Figure 7(b) illustrates the dependence of $\delta_r(B)$ on $l_{H\to B}$ for the case $\xi=f^k(x_c)$.

Let us make an estimate on the χ^2 dependence on $\epsilon\ll 1$. For $\epsilon\ll 1$, the largest contribution to the χ^2 value comes from the first $l_{c,in}(\epsilon)$ images of the hole. If ξ is not eventually periodic, then the first $l_{c,in}(\epsilon)$ wells do not overlap, and the χ^2 value is approximately

$$\chi^2_{\xi\eta}(\epsilon)\simeq\sum_{l'=1}^{l_{c,in}(\epsilon)}\sum_{B\subset f^{l'}(H)}|\delta_r(B)\,\delta(B)|. \tag{14}$$

For $\epsilon\ll 1$, within most of the bins $B\subset f^{l'}(H)$ $(l'<l_{c,in})$, $\mu_N(B)\gg\mu_C(B)$. Therefore, $\delta_r(B)$ is practically independent of ϵ, while $\delta(B)\sim\mu_N(B)\sim\epsilon^{D_{\mu_N}(\xi)}$. Thus, the χ^2-value dependence of ϵ is

$$\chi^2_{\xi\eta}(\epsilon)\sim l_{c,in}(\epsilon)\,\epsilon^{D_{\mu_N}(\xi)}\sim\ln(1/\epsilon)\,\epsilon^{D_{\mu_N}(\xi)}. \tag{15}$$

Figure 8 displays a test of Eq. (15) for the logistic map $(r=3.8)$. The points were fitted to the functional dependence $A_0\ln(1/\epsilon)\epsilon^{A_1}$. As we can see, formula (15) is an excellent fit for the $\chi^2(\epsilon)$ dependence. The fitted value of the exponent A_1 is $A_1=0.46$. The discrepancy from the predicted $A_1=D_{\mu_N}(\xi)=0.5$ value follows from the fact that the approximations we made should hold better for smaller values of ϵ (see Appendix). Note that $\mu_N(H)$ decreases at a faster rate than χ^2 with the decrease of ϵ. This is a consequence of the fact that $l_{c,in}(\epsilon)$ increases with the decrease of ϵ [see Eq. (15)].

If ξ is eventually periodic, than even for small values of ϵ, the images of the hole overlap. Let us evaluate the $\chi^2_{\xi\eta}(\epsilon)$ functional dependence for the case when $f(\xi)=x_F$ $[f(\xi)\neq\xi]$ is an unstable fixed point. In this case, the first $l_{c,in}(\epsilon)-1$ images of the hole are subsets of the image $f^{l_{c,in}(\epsilon)}(H)$. Therefore, $\chi^2\simeq\Sigma_{B\subset f^{l_{c,in}(\epsilon)}(H)}|\delta_r(B)\,\delta(B)|\sim\epsilon^{D_{\mu_N}(\xi)}$. Thus, even if the position of the hole ξ is on an image of the critical point, due to the images of the hole overlap we recover a power-law dependence of the χ^2 value on ϵ. We have checked this relation for $\xi=f^1(x_c), f(\xi)=f^2(x_c)=x_F$, by using the logistic map $f(x)=4x(1-x)$.

When the position of the hole ξ is away from the critical point x_c, then for $\epsilon\ll 1$, the first l_c images of the hole do not start to fold. However, when $\xi=x_c$, then for each ϵ already the first image of the hole is folded. Since the maximum is quadratic, the length of the images $f^l(H)$ is $\sim\epsilon^2$, i.e., the gross differences are observed with the resolution $\eta_{\xi=x_c}=\epsilon^2/\epsilon_B$. It can be shown that local correlations are effectively the same as for the case $\xi=f(x_c)$. Furthermore, if $\eta_{\xi=x_c}=\epsilon^2/\epsilon_B$ is held constant, the χ^2 value has the same functional dependence on ϵ as in the case $\xi=f(x_c)$.

V. CONCLUSION

In conclusion, we have investigated local and global correlations between the naturally invariant measure of the one-dimensional chaotic map f, and the conditionally invariant measure of the transiently chaotic map with a hole f_H. The two measures have been compared on a fine grid with elements of a unit size ϵ_B.

We have demonstrated that the gross differences between the two measures appear within some critical number of the images of the hole H. Two types of gross differences have been reported. We have also demonstrated the existence of fine differences between the two measures, which may occur at the iterates of the critical point.

APPENDIX

In this appendix we study the case $f^k(x_c)=\xi$, $k\geqslant 1$. Consider the bins B that overlap $f^l(H)$, and are to the left of $f^l(\xi)$. By considering the scaling of $\mu_N(B)$ and $\mu_C(B)$ with ϵ, in Sec. IV it is demonstrated that we can find some critical value $\epsilon_c(l)$, such that for $\epsilon<\epsilon_c(l)$, the quantity $\delta_r(B)$ becomes larger than some threshold value p_t close to 1 (e.g., $p_t=0.90$). Let us evaluate the functional dependence $\epsilon_c(l)$ on l.

Consider the bin adjacent to the point $f^l(\xi)$, i.e., B_{in}. The interval $f^{-l}(B_{in})\cap H$ is adjacent to the position of the hole ξ. The length of the interval $f^{-l}(B_{in})\cap H$ is approximately $\epsilon_B/\Lambda^l(\xi)$. Therefore, $\mu_N(f^{-l}(B_{in})\cap H)\simeq c_1(\xi)\times[\epsilon_B/\Lambda^l(\xi)]^{1/2}$. Since ξ is held fixed, $c_1(\xi)$ can be regarded as constant.

The point ξ maps to the point $f^l(\xi)$ in l iterates. Let us denote all other points that map to $f^l(\xi)$ in l iterates by $x_1, x_2, \ldots, x_m$, $\xi \neq x_j$, $j=1,2,\ldots,m$. Since we assume that the spike at $f^l(\xi)$ originates only from the spike at ξ, then $D_{\mu_N}(x_j)=1$, $j=1,2,\ldots,m$. The quantity $\mu_N(f^{-l}(B_{in})\setminus H)$ can be approximately written as $\Sigma_{j=1}^{m}\rho_N(x_j)\epsilon_B/\Lambda^l(x_j)$, where ρ_N denotes the naturally invariant density. Given a map f, the points x_j are determined uniquely by ξ and l. Therefore, we can write $\Sigma_{j=1}^{m}\rho_N(x_j)/\Lambda^l(x_j)=c_2(\xi,l)$.

In the limit $\mu_N(f^{-l}(B_{in})\cap H)/\mu_N(B_{in})=p_t\simeq 1$, equation

$$\mu_N(B_{in})=\mu_N(f^{-l}(B_{in})\cap H)+\mu_N(f^{-l}(B_{in})\setminus H) \quad \text{(A1)}$$

can be approximately written as

$$p_t^{-1}c_1(\xi)\left[\frac{\epsilon_B}{\Lambda^l(\xi)}\right]^{1/2}=c_1(\xi)\left[\frac{\epsilon_B}{\Lambda^l(\xi)}\right]^{1/2}+c_2(\xi,l)\epsilon_B . \quad \text{(A2)}$$

From Eq. (A2) we obtain a functional dependence of $\epsilon_{c,in}$ on l:

$$\epsilon_{c,in}(l)\sim\frac{1}{c_2^2(\xi,l)}\frac{1}{\Lambda^l(\xi)}\sim\frac{1}{c_2^2(\xi,l)}e^{-\lambda(\xi)l}, \quad \text{(A3)}$$

where $\lambda(\xi)$ denotes the Lyapunov exponent obtained for initial condition ξ. Since the points $f^l(\xi)$ bounce around the attractor with increasing l, the quantity $c_2(\xi,l)=\Sigma_{j=1}^{m}\rho_N(x_j)/\Lambda^l(x_j)$ irregularly fluctuates around some average value with increasing l. As an illustration, Fig. 9 displays $c_2(\xi,l)$ and $1/c_2^2(\xi,l)$ for the case $\xi=f^1(x_c)$. Therefore, since $1/\Lambda^l(\xi)$ decreases exponentially fast with increasing l, we conclude that $\epsilon_{c,in}(l)$ decreases very rapidly (approximately exponentially fast) with the increase of l.

By taking the logarithm of Eq. (A3), for sufficiently large l, we approximately write $\lambda(\xi)l \gg 2\ln c_2(\xi,l)$, i.e., $\ln(1/\epsilon_{c,in})\sim\lambda(\xi)l$. From this relation we obtain an expression for the critical number $l_{c,in}(\epsilon)$,

$$l_{c,in}(\epsilon)\sim\frac{1}{\lambda(\xi)}\ln\left(\frac{1}{\epsilon}\right). \quad \text{(A4)}$$

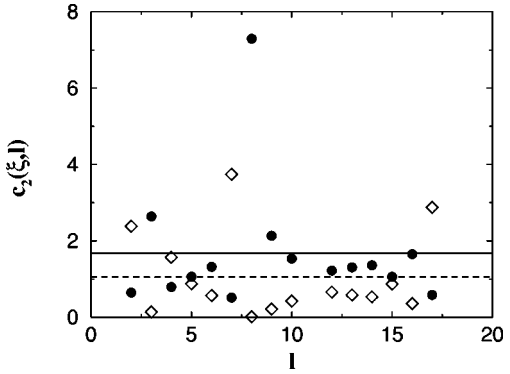

FIG. 9. The quantities $c_2(\xi,l)$ (closed circles) and $1/c_2^2(\xi,l)$ (open diamonds) against l. The position of the hole is $\xi=f^1(x_c)=0.95$. The solid and the dashed lines present the average value of $c_2(\xi,l)$ and $1/c_2^2(\xi,l)$, respectively.

Since relation (A4) is derived from Eq. (A3) for large enough l, Eq. (A4) is approximately valid for small values of ϵ.

Consider the outermost bin B_{out}. We can approximately write $\mu_N(f^{-l}(B_{out})\cap H)\simeq c_1(\xi)(\epsilon/2)^{1/2}-c_1(\xi)(\epsilon/2-\epsilon_B/\Lambda^l(\xi))^{1/2}\simeq c_1(\xi)(\epsilon/2)^{1/2}\eta^{-1}/\Lambda^l(\xi)$. By applying the same strategy as in Eqs. (A1) and (A2), it can be shown that

$$l_{c,out}(\epsilon)\sim\frac{1}{2\lambda(\xi)}\ln\left(\frac{1}{\epsilon}\right), \quad \text{(A5)}$$

i.e., the critical number $l_{c,out}(\epsilon)$ is smaller than $l_{c,in}(\epsilon)$. This is consistent with Fig. 7(b). The increase of both $l_{c,in}(\epsilon)$ and $l_{c,out}(\epsilon)$ with the decrease of ϵ is approximately logarithmical. Unfortunately, relations (A4) and (A5) are derived for so small values of ϵ, that we are unable to check them numerically.

For the bins that are located in between B_{in} and B_{out}, the critical value $\epsilon_c(l)$ is $\epsilon_{c,out}(l)\leq\epsilon_c(l)\leq\epsilon_{c,in}(l)$. Furthermore, the critical number $l_c(\epsilon)$ corresponding to these bins is $l_{c,out}(\epsilon)\leq l_c(\epsilon)\leq l_{c,in}(\epsilon)$. This is consistent with Figs. 7(a) and 7(b).

[1] E. Ott, *Chaos in Dynamical Systems* (Cambridge University Press, Cambridge, 1993).

[2] J.P. Eckmann and D. Ruelle, Rev. Mod. Phys. **57**, 617 (1985).

[3] R. Shaw, Z. Naturforsch. A **36A**, 80 (1981).

[4] M. Misiurewicz, Publ. Math. **53**, 17 (1981); M. Benedicks and M. Misiurewicz, *ibid.* **69**, 203 (1989); M.V. Jacobson, Commun. Math. Phys. **81**, 39 (1981); D. Ruelle, *ibid.* **55**, 47 (1977).

[5] P. Collet and J.P. Eckmann, *Iterated Maps on the Interval as Dynamical Systems* (Birkhäuser, Boston, 1980).

[6] C. Grebogi, E. Ott, and J.A. Yorke, Phys. Rev. A **37**, 1711 (1988); Y.-C. Lai, Y. Nagai, and C. Grebogi, Phys. Rev. Lett. **79**, 649 (1997); Y.-C. Lai, Phys. Rev. E **56**, 6531 (1997).

[7] T. Ogawa, Phys. Rev. A **37**, 4286 (1988).

[8] T. Tél, in *Directions in Chaos*, edited by Hao Bai-lin (World Scientific, Singapore, 1990), Vol. 3, p. 149.

[9] T. Tél, Phys. Rev. A **36**, 1502 (1987); P. Szépfalusy and T. Tél, *ibid.* **34**, 2520 (1986); T. Tél, Phys. Lett. A **119**, 65 (1986); H. Lustfeld and P. Szépfalusy, Phys. Rev. E **53**, 5882 (1996); A. Csordás, G. Györgyi, P. Szépfalusy, and T. Tél, Chaos **3**, 31 (1993).

[10] M. Dhamala and Y.-C. Lai, Phys. Rev. E **60**, 6176 (1999).

[11] H. Kantz and P. Grassberger, Physica D **7**, 75 (1985).

[12] C. Grebogi, E. Ott, and J.A. Yorke, Phys. Rev. Lett. **57**, 1284 (1986); C. Grebogi, E. Ott, F. Romeiras, and J.A. Yorke, Phys. Rev. A **36**, 5365 (1987).

[13] J. Jacobs, E. Ott, and C. Grebogi, Physica D **108**, 1 (1997).

[14] G. Pianigiani and J.A. Yorke, Trans. Am. Math. Soc. **252**, 351 (1979); G. Pianigiani, J. Math. Anal. Appl. **82**, 75 (1981).

[15] N. Chernov and R. Markarian, Bol. Soc. Bras. Math. **28**, 271 (1997); **28**, 315 (1997); N. Chernov, R. Markarian, and S. Troubetzkoy, Ergod. Theory Dyn. Syst. **18**, 1049 (1998); **20**, 1007 (2000).

[16] P. Collet, S. Martinez, and B. Schmitt, Nonlinearity **7**, 1437 (1994); P. Collet, S. Martinez, and V. Maume-Deschamps, *ibid.* **13**, 1263 (2000).

[17] A. Lopes and R. Markarian, SIAM (Soc. Ind. Appl. Math.) J. Appl. Math. **56**, 651 (1996).

[18] J. Jacobs, E. Ott, and B.R. Hunt, Phys. Rev. E **57**, 6577 (1998).

[19] E. Bollt, Y.-C. Lai, and C. Grebogi, Phys. Rev. Lett. **79**, 3787 (1997); E. Bollt and Y.-C. Lai, Phys. Rev. E **58**, 1724 (1998); Y.-C. Lai, E. Bollt, and C. Grebogi, Phys. Lett. A **255**, 75 (1999); M. Dolnik and E. Bollt, Chaos **8**, 702 (1998).

[20] K. Zyczkowski and E.M. Bollt, Physica D **132**, 392 (1999).

[21] V. Paar and N. Pavin, Phys. Rev. E **55**, 4112 (1997); Phys. Lett. A **235**, 139 (1997).

[22] H. Buljan and V. Paar, Phys. Rev. E **63**, 066205 (2001); V. Paar and H. Buljan, *ibid.* **62**, 4869 (2000).

[23] F. Hunt, SIAM (Soc. Ind. Appl. Math.) J. Appl. Math. **50**, 307 (1990).

[24] The χ^2 value defined in Eq. (4) resembles the definition of the χ^2 test that is often used in statistics. Note that the definition of the χ^2 value utilizes the *relative* frequencies [$\mu_N(B)$ and $\mu_C(B)$].

[25] T. Shinbrot, E. Ott, C. Grebogi, and J.A. Yorke, Phys. Rev. Lett. **65**, 3215 (1990).